THE JOURNAL OF PHYSICAL CHEMISTRY B

ARTICLE

pubs.acs.org/JPCB

Effects of Temperature and Salt Concentration on the Structural and Dynamical Features in Aqueous Solutions of Charged Triblock Copolymers

Anna-Lena Kjøniksen,[†,‡] Kaizheng Zhu,[†] Manja A. Behrens,[§] Jan Skov Pedersen,[§] and Bo Nyström*[,†]

[†]Department of Chemistry, University of Oslo, P.O. Box 1033, Blindern, N-0315 Oslo, Norway

[‡]Department of Pharmaceutics, School of Pharmacy, University of Oslo, P.O. Box 1068, Blindern, N-0316, Oslo, Norway

[§]Department of Chemistry and iNANO Interdisciplinary NanoScience Center, Aarhus University, Langelandsgade140, DK-8000 Århus C, Denmark

ABSTRACT: Effects of temperature and salt addition on the association behavior in aqueous solutions of a series of charged thermosensitive methoxypoly(ethylene glycol)-*block*-poly(*N*-isopropylacrylamide)-*block*-poly(4-styrenesulfonic acid sodium) triblock copolymers ($MPEG_{45}$-*b*-$P(NIPAAM)_n$-*b*-$P(SSS)_{22}$) with different lengths of the PNIPAAM block (n = 17, 48, and 66) have been studied with the aid of turbidity, small-angle X-ray scattering (SAXS), and dynamic light scattering (DLS). Increasing temperature and salinity as well as longer PNIPAAM blocks are all factors that promote the formation of association structures. The SAXS data show that, for the copolymers with n = 48 and n = 66, increasing temperature and salt concentration induce interchain associations and higher values of the aggregation number, whereas no aggregation was observed for the copolymer with the shortest PNIPAAM chain. However, DLS measurements reveal the presence of larger association clusters. The cloud point is found to decrease with raising salinity and longer PNIPAAM block. The general picture that emerges is the delicate interplay between repulsive electrostatic forces and hydrophobic interactions and that this balance can be tuned by changing the temperature, salinity, and the length of the PNIPAAM block.

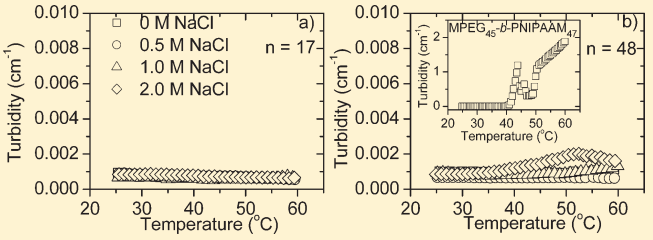

INTRODUCTION

The temperature-induced self-assembly of amphiphilic block copolymers has attracted a great deal of interest[1−12] not only because of its fundamental importance as related to polymer nanostructures but also as model systems for various biological applications such as protein folding and drug release formulations. Poly(*N*-isopropylacrylamide) (PNIPAAM) is a typical paradigm of a thermosensitive water-soluble polymer that exhibits a lower critical solution temperature (LCST) around 32 °C,[13] below which the polymer is soluble and above which the molecules are in a collapsed state and the system approaches macroscopic phase separation. In a recent paper[14] on low-molecular-weight samples ($M_w < 1.2 \times 10^4$) of aqueous PNIPAAM, it was shown that the value of LCST decreases when the molecular weight and/or polymer concentration rises. It was concluded that the temperature-induced intermolecular associations are most intensive for the PNIPAAM sample with the longest chains.

The strength of the temperature-induced association tendency of PNIPAAM in aqueous solution can be modulated by using amphiphilic copolymers containing PNIPAAM and a hydrophilic block. This type of copolymer usually undergoes micellization when the block copolymer is dissolved in a selective solvent for one of the blocks.[7] In this process, the unimers tend to self-assemble into micelle-like structures at very low polymer concentrations, and the supramolecular structure that is formed consists of a hydrophilic corona and a hydrophobic core.[7] In a recent investigation,[8] a thermoresponsive methoxypoly(ethylene glycol)-*block*-poly(*N*-isopropylacrylamide) ($MPEG_{53}$-*b*-$PNAPAAM_{113}$) diblock copolymer was synthesized, and this polymer exhibits a LCST that is significantly higher than for the corresponding PNIPAAM polymer because of the hydrophilic MPEG block. The micelles that are formed from this copolymer are characterized by large hydrophobic cores and relatively thin hydrophilic shells, and they may be called "crew-cut" micelles.[9,15] The results revealed an intricate interplay between temperature-induced intermicellization and shrinking of the species at intermediate temperatures and the formation of large intermicellar complexes at high temperatures.[16] To improve the stability of the species they can be decorated with charges, and the properties of these micelles can be modulated by temperature change and addition of salt.

In this work, we have synthesized a series of thermosensitive methoxypoly(ethylene glycol)-*block*-poly(*N*-isopropylacrylamide)-*block*-poly(4-styrenesulfonic acid sodium) triblock copolymers by utilizing atom transfer radical polymerization (ATRP).[17,18] The products obtained from the synthesis have the following composition: $MPEG_{45}$-*b*-$P(NIPAAM)_n$-*b*-$P(SSS)_{22}$. To explore the

Received: August 11, 2010
Revised: December 20, 2010
Published: February 22, 2011

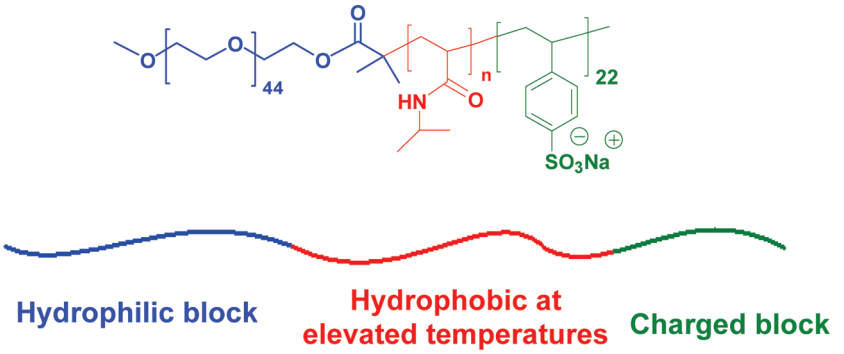

Figure 1. Chemical structure and properties of the synthesized block copolymers.

association features of this anionic triblock copolymer, three samples have been prepared with n = 17, 48, and 66. The chemical structure and characteristic data of the triblock copolymer are displayed in Figure 1.

The idea is that the strength of hydrophobic interaction at elevated temperatures is enhanced as the length of the PNIPAAM block is increased. The aim of this investigation is to gain insight into the delicate interplay between electrostatic interactions and hydrophobic interactions at different temperatures and levels of salt addition, and how these changes affect the structure and dynamics of these copolymers. For this purpose, we have carried out turbidity, small-angle X-ray scattering (SAXS), and dynamic light scattering (DLS) experiments on 1 wt % solutions of $MPEG_{45}$-*b*-$P(NIPAAM)_n$-*b*-$P(SSS)_{22}$ at various temperatures and different levels of salt (NaCl) addition. The detailed structural and dynamical features obtained from this investigation provide us with a better understanding of the delicate competition between hydrophobic associations and electrostatic interactions in systems of thermally sensitive charged copolymers. This study discloses some novel structural and dynamical findings in systems that form intermicellar structures at elevated temperatures.

EXPERIMENTAL SECTION

Materials. *N*-Isopropylacrylamide (NIPAAM, Acros) was recrystallized from a toluene/hexane mixture solvent and dried at room temperature under vacuum prior to use. Copper(I) chloride from Aldrich was washed with glacial acetic acid, followed by washing with methanol and ethyl ether to remove impurities, and then dried under vacuum and kept under N_2 atmosphere. *N*,*N*,*N*′,*N*″,*N*‴,*N*‴′-Hexamethyltriethylenetetramine (Me_6TREN) was prepared according to a procedure described elsewhere.[19] *N*,*N*′-Dimethylformamide and triethylamine was distilled under vacuum prior to use. All the others chemicals from Aldrich and Fluka were used as received. The synthesis of the MPEG macroinitiator was performed in accordance with a published procedure by the reaction of monomethoxyl-capped poly(ethylene glycol) ($MPEG_{45}$−OH and the data of M_n = 2000 was provided by the manufacturer) with 2-bromoisobutyryl bromide in the presence of triethylamine.[20] The water employed in this investigation was purified with a Millipore Milli-Q system, and the resistivity was approximately 18 MΩ cm.

Copolymer Synthesis. The anionic triblock copolymers M-$(PEG)_{45}$-*b*-$P(NIPAAM)_n$-*b*-$P(SSS)_{22}$ were synthesized via a simple "one-pot" two steps ATRP,[17,18,21] which was carried out in a water/DMF, 50:50 (v/v), mixture solvent at 25 °C and with MPEG-MI/CuCl/$CuCl_2$/Me_6TREN = 1/1/0.6/1.6 (molar ratio) as the initiator/catalyst system. The details of the preparation and purification of these copolymers were conducted under similar conditions as described in our previous papers.[8,9,14,22] The synthesis route of $M(PEG)_{45}$-*b*-$P(NIPAAM)_n$-*b*-$P(SSS)_{22}$ is displayed in Scheme 1. In a general procedure, NIPAAM (55 mmol, 6.22 g) and MPEG-MI (1 mmol, 2.13 g) were dissolved in 25 mL of a water/DMF 50:50 (v/v) solvent mixture ([NIPAAM] = 2.0 M) in a 50 mL Schlenk flask under magnetic stirring. The mixture was degassed by bubbling with argon for at least 1 h, before it was immersed in a water bath that was kept at about 25 °C. A volume of 2 mL of the freshly

Scheme 1. Synthesis Route for the Preparation of the MPEG-*b*-PNIPAAM-*b*-PSSS Triblock Copolymers via "One-Pot" Two Steps ATRP

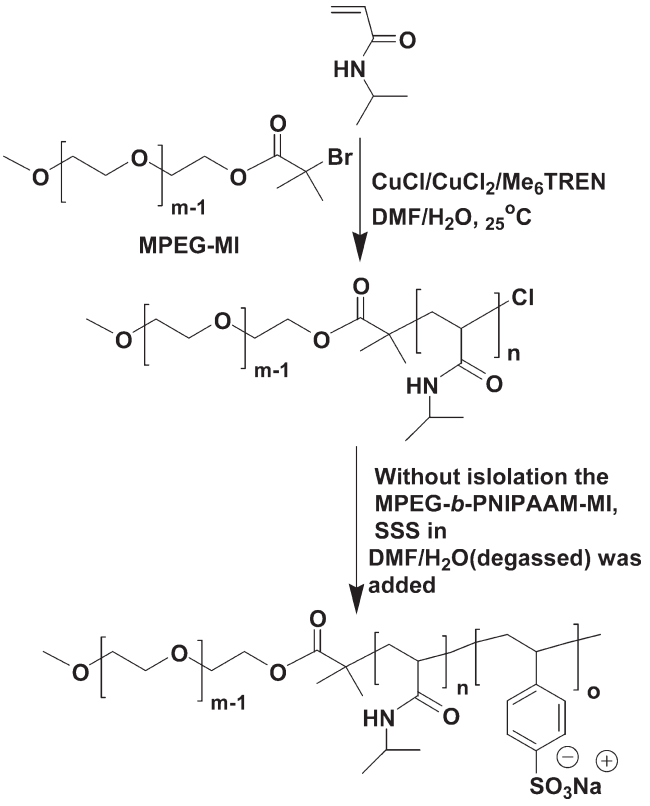

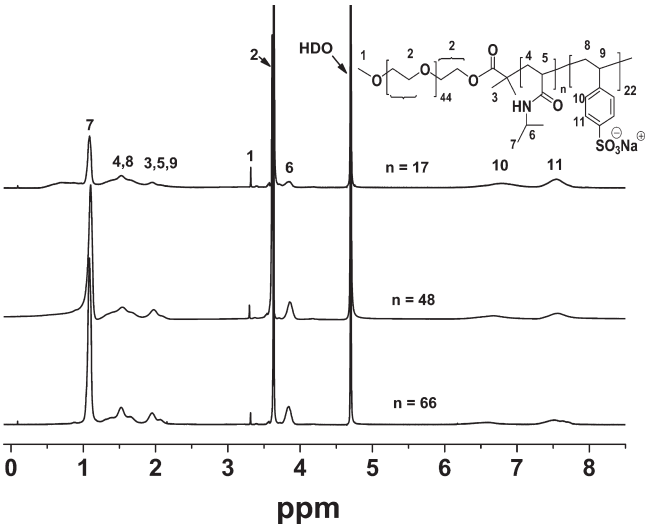

Figure 2. ^{1}H NMR spectra of the synthesized MPEG-*b*-PNIPAAM-*b*-PSSS triblock copolymers in D_2O (300 MHz).

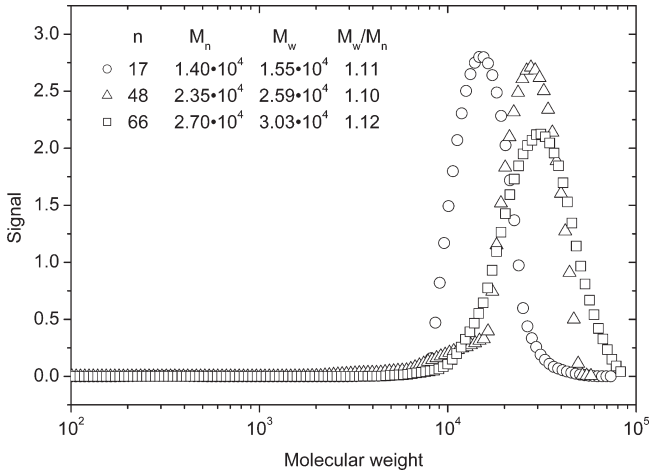

Figure 3. Molecular weight distribution curves of the $MPEG_{45}$-*b*-$P(NIPAAM)_n$-*b*-$P(SSS)_{22}$ samples in dilute aqueous solutions (0.01 M NaCl) with the aid of AFFFF.

prepared Cu(I)−Cu(II)−Me_6TREN water stock solution (prepared by adding degassed water (6.3 mL) to CuCl (4 mmol, 0.396 g), $CuCl_2$ (2.4 mmol, 0.32 g), and Me_6TREN (6.4 mmol, 1.7 mL) exposed to vigorous stirring under the influence of argon flow) was withdrawn via a degassed syringe and quickly added to the above mixture; the polymerization reaction was then initiated. When the NIPAAM monomer conversion reached approximately 90% (after approximately 25 min), ^{1}H NMR analysis indicated that more than 90% of the NIPAAM had been polymerized (disappearance of the vinyl signals at δ = 5.5—6.0 ppm), a well-degassed solution of anionic monomer SSS in a water/DMF (80/20, v/v) mixture was then added quickly ([SSS]/[MPEG-MI] = 40/1) to the reaction mixture via a syringe under an atmosphere of argon. After 1 h, the polymerization was stopped by exposing it to air, and the sample was diluted with water and further dialyzed first against 0.1 N NaCl and then against distilled water for at least 3 weeks (to remove the salt) using a regenerated cellulose dialysis membrane with a molecular weight cutoff of 8000. The white solid triblock copolymer MPEG-*b*-PNIPAAM-*b*-PSSS was then finally isolated by lyophilization.

Characterization of the Triblock Copolymers. The chemical structure and composition of the triblock copolymers were ascertained by their ^{1}H NMR spectra (Figure 2) with a Bruker AVANCE DPX 300 NMR spectrometer (Bruker Biospin, Fällanden, Switzerland), operating at 300.13 MHz at 25.0 °C by using heavy water (D_2O) as the solvent. The ^{1}H chemical shift in D_2O is referred to the residual HDO proton (δ = 4.70 ppm) in D_2O. The number-average molecular weight and the unit numbers of *m*, *n* and *o*, in $MPEG_m$-*b*-$P(NIPAAM)_n$-*b*-$P(SSS)_o$ were then evaluated by comparing the integral area of the end-capped methoxyl proton peak (**1**) of MPEG (δ = 3.30 ppm), the methyne proton peak (**6**) of PNIPAAM (δ = 3.85 ppm), and the aryl proton (**10, 11**) of PSSS (δ = 6.6 ppm and δ = 7.5 ppm) obtained from their NMR spectrum (Figure 2). We have successfully synthesized three triblock copolymers $M(PEG)_m$-*b*-$P(NIPAAM)_n$-*b*-$P(SSS)_o$ with different lengths of the NIPAAM (*n* = 17, *n* = 48, and *n* = 66) block, but keeping the same numbers of PEG and anionic SSS units in the copolymers, by carefully adjusting the molar ratio of NIPAAM with the MPEG macroinitiator as well as the polymerization time. The monomer/initiator (NIPAAM/SSS/MPEG-MI, molar ratio) are 25/40/1, 55/40/1, and 75/40/1 for the samples with *n* = 17, *n* = 48, and *n* = 66 of NIPAAM units, respectively. The compositions of the triblock copolymers are estimated to be *m*/*n*/*o* = 45/17/22, 45/48/22, and 45/66/22.

Asymmetric Flow Field-Flow Fractionation. The AFFFF experiments[8,23] were conducted on an AF2000 FOCUS system (Postnova Analytics, Landsberg, Germany) equipped with an RI detector (PN3140, Postnova) and a multiangle (7 detectors in the range 35−145°) light scattering detector (PN3070, λ = 635 nm, Postnova). The $MPEG_{45}$-*b*-$P(NIPAAM)_n$-*b*-$P(SSS)_{22}$ samples (1.0 wt % in 0.01 M NaCl) were measured using a 350 μm spacer, a regenerated cellulose membrane with a cutoff of 1000 (Z-MEM-AQU-425N, Postnova), and an injection volume of 20 μL. The measurements were performed by employing a constant detector flow rate of 1.0 or 0.7 mL/min. The focusing time was 6 min at a cross flow of 4 mL/min for *n* = 17 and 6 min at a cross flow of 3 mL/min for *n* = 48, and 15 min at a cross flow of 4 mL/min for *n* = 66. The cross flow was then linearly reduced to zero during a period of time of 10−20 min depending on the sample. Processing of the measured data was achieved by the Postnova software (AF2000 Control, version 1.1.011). The molecular weights of the samples were determined using this software with a Zimm-type fit, and a refractive index increment (d*n*/d*c*) of 0.150 for *n* = 17, 0.158 for *n* = 48, and 0.157 for *n* = 66 (determined by using the RI detector at 32 °C). The experiments were carried out at 25 °C for the samples with *n* = 17 and *n* = 48. However, due to association effects the measurements on the copolymer with *n* = 66 were performed at a much lower temperature (10 °C) to suppress the aggregation effects at elevated temperatures. The results reveal that the triblock copolymers have fairly narrow molecular weight distributions (see Figure 3) with polydispersity indices (M_w/M_n) of approximately 1.1. All samples used for the experiments described in the following were prepared by weighing the components and the solutions were homogenized by stirring for 1 day at ambient temperature.

Turbidimetry. Influence of temperature on the transmittance of aqueous solutions of the studied $MPEG_{45}$-*b*-$P(NIPAAM)_n$-*b*-$P(SSS)_{22}$ samples was measured with a NK60-CPA cloud point

analyzer from Phase Technology, Richmond, BC, Canada. A detailed description of the equipment and determination of turbidities have been given elsewhere.[5] This apparatus utilizes a scanning diffusive technique to characterize phase changes of the samples with high sensitivity and accuracy. The light from an AlGaAs light source, operating at 654 nm, was focused on the measuring sample that was applied onto a specially designed glass plate that is coated with a thin metallic layer of very high reflectivity (mirror). Directly above the sample, an optical system with a light-scattering detector continuously monitors the scattered intensity signal (S) of the solution as it is subjected to prescribed temperature alterations. The relationship between the signal and the turbidity (τ) is given by the following empirical expression $\tau\ (\mathrm{cm}^{-1}) = 9.0 \times 10^{-9} S^{3.751}$.[5] The results from the instrument will be expressed in terms of turbidity. The heating rate was set to 0.2 °C/min. The temperature at which the first deviation of the scattered intensity from the baseline occurred was taken as the cloud point of the considered sample.

Small-Angle X-ray Scattering. The experiments were conducted on the SAXS instrumentation at the University of Aarhus.[24] The apparatus is the prototype of the NanoSTAR instrument commercially available from Bruker AXS. The camera consists of a rotating anode (Cu, $0.1 \times 0.1\ \mathrm{mm}^2$ effective source point, 0.96 kW power) and a three-pinhole collimation optimized with respect to flux and background, and therefore optimal for scattering from solutions. The Cu Kα radiation is monochromatic and made parallel by two side-by-side Göbel mirrors. Data collection was conducted over an extended temperature domain (20−90 °C) in a reusable thermostated quartz capillary, which is placed in the integrated vacuum chamber of the camera. The quartz capillary is glued into a home-built capillary holder with good thermal contact to the temperature-controlled block that employs a Peltier element (Anton Paar GmbH, Austria). The instrument configuration gives access to a range of scattering vectors q between 0.01 and 0.33 $\mathrm{Å}^{-1}$. The modulus of the scattering vector is given by $q = (4\pi n/\lambda)\sin(\theta/2)$, where n is the refractive index which for all practical purposes equals unity for the X-rays, θ is the scattering angle, and λ is the wavelength. The two-dimensional data sets are recorded using a two-dimensional position-sensitive gas detector (HiSTAR). The spectra from all solutions were isotropic and the data were azimuthally averaged, corrected for variations in detector efficiency and for spatial distortions. The background scattering from solvent was subtracted, and the scattering intensities were transformed to absolute units using the scattering of water as a standard.[25] Measurement time was 1 h at each temperature. Due to long time of data accumulation, the SAXS measurements were carried out at a number of fixed temperatures.

Theory and Data Analysis. Although PNIPAAM is generally considered to be relatively hydrophilic at low temperatures, previous studies have shown that aggregates are observed to coexist with single molecules even at temperatures substantially below the LCST.[14] However, in the absence of salt no large aggregates are observed by SAXS for the considered triblock copolymers at low temperatures, indicating that only single molecules are probed at these conditions. With 0.5 M NaCl, the scattering data are similar to the curves expected for nonionic flexible polymers and there are no clear indications of interchain correlations or micellation. Therefore, models of flexible polymer chains were fitted to these data with the purpose of extracting radius of gyration R_g. Results for this parameter allows us to check if we have nonassociated chains and to estimate the Kuhn length b, which can be considered as the equivalent step length of a random walk of the same length. For the lower molecular weights, the form factor of a Gaussian chain could be used[26]

$$P(q) = 2[\exp(-u) + u - 1]/u^2 \tag{1}$$

where

$$u = \langle R_g^2 \rangle q^2 \tag{2}$$

and $\langle R_g^2 \rangle$ is ensemble average of the square of the radius of gyration. $\langle R_g^2 \rangle$ can thus be obtained directly through a least-squares fitting procedure.[27,28] The radius of gyration can further be related to the contour length L of the chains and the Kuhn length b by

$$\langle R_g^2 \rangle = (Lb)/6 \tag{3}$$

For the copolymer with highest molecular weight the Gaussian model did not provide satisfactory fits as the decay of the data was slower than predicted by the model. This was ascribed to excluded volume effects which change the limiting power law from q^{-2} to $q^{-1.58}$. For these data the model expression developed by Pedersen and Schurtenberger[29] which take into account excluded volume effects was used.

For the data at higher temperatures, significant increase in the scattering at low q was observed and this can be ascribed to micelle formation. In order to obtain information on the size of these and their aggregation numbers, indirect Fourier transformations were performed. The scattering intensity is related to the real space function know as the pair distance distribution functions $p(r)$

$$I(q) = 4\pi \int_0^\infty p(q) \frac{\sin(qr)}{qr}\, \mathrm{d}r \tag{4}$$

where

$$p(r) = r^2 \langle \int \Delta\rho(\mathbf{r}' - \mathbf{r}) \Delta\rho(\mathbf{r}')\, \mathrm{d}\mathbf{r}' \rangle_\Omega \tag{5}$$

In this equation, $\Delta\rho(\mathbf{r})$ is the excess scattering length distribution and $\langle ... \rangle_\Omega$ means averaging over orientations. For particulate systems, $p(r)$ represents the ensemble average function of the individual particles and thus yields information about the overall size and shapes of the polymer species. The function goes to zero at the maximum diameter of the particles D_{max} and has certain characteristic shapes for different micellar morphologies.

The distance distribution functions were obtained from an indirect Fourier transformation (IFT).[30] In this procedure, $p(r)$ is expressed as a sum of cubic b spline functions[31] which allow free-form determination of the function

$$p(r) = \sum_{i=1}^{m} a_i B_i(r) \tag{6}$$

where a_i are coefficients to be determined in the fit and $B_i(r)$ are the bell-shaped cubic b splines. The Fourier transformations of the spline functions are fitted to the experimental data using a least-squares procedure that also employs a smoothness constraint for numerical stability of the solutions. The approach is implemented in homemade software and can be applied to solutions both with (WGIFT) and without (WIFT) a structure factor that accounts for interparticle interactions (C. L. P. Oliveira and J. S. Pedersen, unpublished work).

The $p(r)$ function obtained from IFT provides also evaluation of the radius of gyration and the forward scattering as, respectively

$$\langle R_g^2 \rangle = \frac{\int_0^\infty p(r) r^2 \, dr}{2\int_0^\infty p(r) \, dr} \tag{7}$$

and

$$I(q = 0) = 4\pi \int_0^\infty p(r) \, dr \tag{8}$$

If it is assumed that we have nonassociated chains at 20 °C and that the contrast factor of the polymers is temperature independent, the apparent aggregation number N_{agg} of the block copolymer in the solution can be determined from the following expression

$$N_{agg} \approx I_x(q = 0)/I_{20°C}^{\text{no salt}}(q = 0) \tag{9}$$

where $I_x(q=0)$ is the scattered intensity of the measured solution at $q = 0$ and the denominator represents the forward scattered intensity at a reference condition. The expression for the aggregation number yields only an estimate of the aggregation number because it is difficult to estimate the correct forward scattering for the reference state. For example, the forward scattering at 20 °C in the absence of salt was calculated using the generalized indirect Fourier transformation, where the interparticle interactions are accounted for through the structure factor, and it is difficult to estimate the accuracy of this procedure. Another shortcoming of the approach is the assumption of temperature-independent contrast factors. Values for apparent partial specific densities of blocks of the polymer as a function of temperature can be used for estimating the variation of the contrast factor. However, we do not have values for the PSSS block, but the measured values of the apparent partial specific density of PEG[32] and PNIPAAM[33] allow us to estimate the variation of the contrast factor between 20 and 90 °C for these two blocks using a linear extrapolation of the density of PNIPAAM to 90 °C. For both blocks the square of the excess electron density changes by about a factor of 2. This means that, with the applied procedure, we are underestimating the aggregation number by about a factor of 2 at high temperature. Since our main interest is focused on the changes of N_{agg} with temperature and salt addition and not the absolute value, we believe that this procedure yields a good impression of the actual behavior.

Dynamic Light Scattering. Dynamic light scattering (DLS) experiments were carried out by means of an ALV/CGS-8F multidetector version compact goniometer system, with eight fiber-optical detection units, from ALV-GmbH, Langen, Germany. The beam from a Uniphase cylindrical 22 mW HeNe laser, operating at a wavelength of 632.8 nm with vertically polarized light, was focused on the sample cell (10 mm NMR tubes, Wilmad Glass Co., of highest quality) through a temperature-controlled cylindrical quartz container (with two plane-parallel windows), which is filled with a refractive index matching liquid (*cis*-decalin). The temperature in the container is controlled to within ±0.01 °C with a heating/cooling circulator. The polymer solutions were filtered in an atmosphere of filtered air through a 5 μm filter (Millipore) directly into precleaned NMR tubes. The DLS experiments were performed with a temperature variation (0.2 °C/min) as for the turbidity measurements. The correlation function data were recorded continuously with an accumulation time of 1 min. This accumulation time was chosen to be a compromise between the time needed to accumulate good correlation functions without too much noise in the data, while at the same time keeping the accumulation time short enough to avoid significant temperature-induced changes in the sample during the accumulation of each correlation function. Sometimes this compromise made it difficult to gain good correlation functions all the way down to the baseline. The DLS experiments were conducted with the same protocol as the turbidity measurements.

In the solutions of these copolymers, the experimentally recorded intensity autocorrelation function $g^2(q,t)$ is directly linked to the theoretically amenable first-order electric field autocorrelation $g^1(q,t)$ through the Siegert[34] relationship $g^2(q, t) = 1 + B|g^1(q,t)|^2$, where B (≤ 1) is an instrumental parameter.

Most of the correlation function can be described by the sum of two stretched exponentials

$$g^1(t) = A_f \exp[-(t/\tau_{fe})^\gamma] + A_s \exp[-(t/\tau_{se})^\beta] \tag{10}$$

with $A_f + A_s = 1$. The parameters A_f and A_s are the amplitudes for the fast and the slow relaxation time, respectively. The variables τ_{fe} and τ_{se} are the relaxation times characterizing the fast and the slow process, respectively. In some cases when the fraction of large species dominates, the correlation functions could be fitted with a single stretched exponential ($g^1(t) = \exp[-(t/\tau_{se})^\beta]$).

A bimodal relaxation process has recently been reported[5,9,35,36] from DLS studies on associating polymer systems of various natures. In the analysis of the correlation functions by means of eq 10, a nonlinear fitting algorithm was employed to obtain best-fit values of the parameters A_f, τ_{fe}, τ_{se}, γ, and β appearing on the right-hand side of eq 10.

The fast mode is always diffusive (q^2-dependent) and it yields the mutual diffusion coefficient D ($\tau_f^{-1} = Dq^2$) of unimers or micelles. The slow mode (the second term on the right-hand side of eq 10) characterizes the dynamics of large clusters or intermicellar structures and this mode exhibits typically a stronger q-dependence than a diffusive process. The results suggest two types of species, and the stretched exponential nature of both the fast and the slow mode indicates that both populations of entities contain particles of different sizes. Depending on polymer concentration and temperature, it is expected that an aqueous solution of $MPEG_{45}$-*b*-$P(NIPAAM)_n$-*b*-$P(SSS)_{22}$ contains various types of species, such as unimers, micelles, and intermicellar structures. High temperature and high polymer concentration promote the growth of the intermicellar complexes, especially for solutes of high hydrophobicity.

The parameters τ_{fe} and τ_{se} in eq 10 are effective relaxation times, and β ($0 < \beta \leq 1$) and γ ($0 < \gamma \leq 1$) are measures of the widths of the distributions of relaxation times. The mean relaxation time for the fast and slow mode is given by

$$\tau_f = \frac{\tau_{fe}}{\gamma} \Gamma\left(\frac{1}{\gamma}\right) \tag{11a}$$

$$\tau_s = \frac{\tau_{se}}{\beta} \Gamma\left(\frac{1}{\beta}\right) \tag{11b}$$

where $\Gamma(x)$ is the gamma function. In this study, we found that depending on the stage of aggregation, the values of β and γ are in the intervals 0.3−1.0 and 0.8−1.0, respectively.

Since the fast relaxation mode always is diffusive ($D = (1/\tau_f)/q^2$) for the considered systems, the apparent hydrodynamic radii R_h

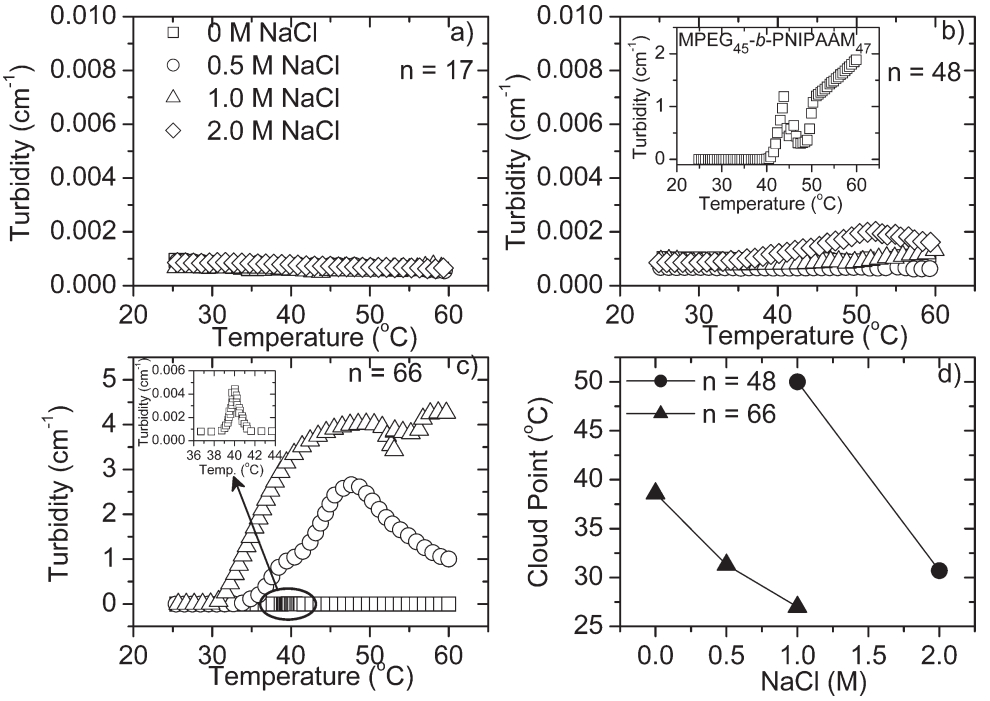

Figure 4. Temperature dependences of the turbidity during a heating rate of 0.2 °C/min of 1 wt % solutions of $M(PEG)_{45}$-*b*-$P(NIPAAM)_n$-*b*-$P(SSS)_{22}$ at different levels of salt addition. The inset in panel (c) shows a magnification of the transition region, and the inset in (b) displays the turbidity of a corresponding diblock without the charged block. (d) Effects of PNIPAAM length and salt concentration on the cloud point.

of the species can be calculated by using the Stokes−Einstein relationship

$$R_h = \frac{k_B T}{6\pi\eta D} \tag{12}$$

where k_B is the Boltzmann constant, T is the absolute temperature, η is the viscosity of the solvent, and D is the mutual diffusion coefficient.

All experiments were carried out at a fixed polymer concentration of 1 wt %, where micelles are formed and elevated temperature and enhanced hydrophobicity favor the formation of intermicellar structures. The overlap concentration, c^*, can be estimated from[37] $c^* = (3M)/(4\pi N_A R_h^3)$, where M is the molecular weight, N_A is Avogadro's constant, and R_h is the hydrodynamic radius. Using this equation at 25 °C for the solutions without salt, we find that $c^* > 9$ wt % for the copolymers used in this study. The polymer concentration of 1 wt % that is utilized in this work is therefore well into the dilute regime. However, due to the finite concentration and the relatively strong electrostatic interactions for the salt-free solution, the derived values of R_h are to some extent influenced by interaction effects and it will therefore be termed "apparent". Theoretically, the effects on the diffusion constant can at low concentration be described by[38,39] $D_{app} = D(1 + k_D c)$, where $k_D = 2A_2M_w - k_f - 2v$. In this expression, A_2 is the second virial coefficient, M_w is the molecular weight, k_f is the frictional coefficient, and v is the partial specific volume of the particle. In general, for strong repulsion, k_D is positive, and thus the apparent R_h is smaller than at infinite dilution.

RESULTS AND DISCUSSION

In solutions of amphiphilic copolymers the micellization process is governed by the critical micelle concentration (cmc) and the critical micelle temperature (cmt), and at higher polymer concentrations and/or elevated temperatures intermicellar complexes are promoted.[40,41] Usually, the cmc is very low for many copolymers and it can be difficult to determine it with conventional experimental techniques. For the triblock copolymers considered in this work at a fixed polymer concentration, the formation of temperature-induced supramolecular structures is promoted by a long PNIPAAM block and addition of salt.

Turbidimetry. The turbidity of spherical particles with a concentration c and a radius R can be expressed as[42]

$$\tau = 3cQ_{ext}/(4R\rho) \tag{13}$$

where Q_{ext} is the Mie extinction efficiency and ρ is the density of the particles. For spherical particles with a mass m and a volume $V_p = (4/3)\pi R^3$, we can substitute $\rho = m/V_p$ and $c = N_p m/V_s$ (N_p is the number of particles, and V_s is the volume of the sample) into (13):

$$\tau = Q_{ext}N_p\pi R^2/V_s \tag{14}$$

The parameter Q_{ext} is a function of the relative refractive index, n_p/n_0, where n_p is the refractive index of the particle and n_0 is the refractive index of the solvent. Q_{ext} increases with increasing values of n_p/n_0.[42] For a polymer cluster that is swollen in water, n_p/n_0 is close to unity (cluster consist mainly of water), while for a more compact polymer cluster (containing little water), n_p/n_0 is significantly larger. Consequently, in addition to increasing with the number and size of the particles, the turbidity of a sample increases with the compactness of the species. This effect has been observed previously for PNIPAAM microgels.[43]

Temperature dependences of the turbidity for 1 wt % solutions of $M(PEG)_{45}$-*b*-$P(NIPAAM)_n$-*b*-$P(SSS)_{22}$ at different salt concentrations are depicted in Figure 4. We note that the turbidity for solutions of the triblock copolymer with the shortest

dx.doi.org/10.1021/jp1075884 |J. Phys. Chem. B 2011, 115, 2125–2139

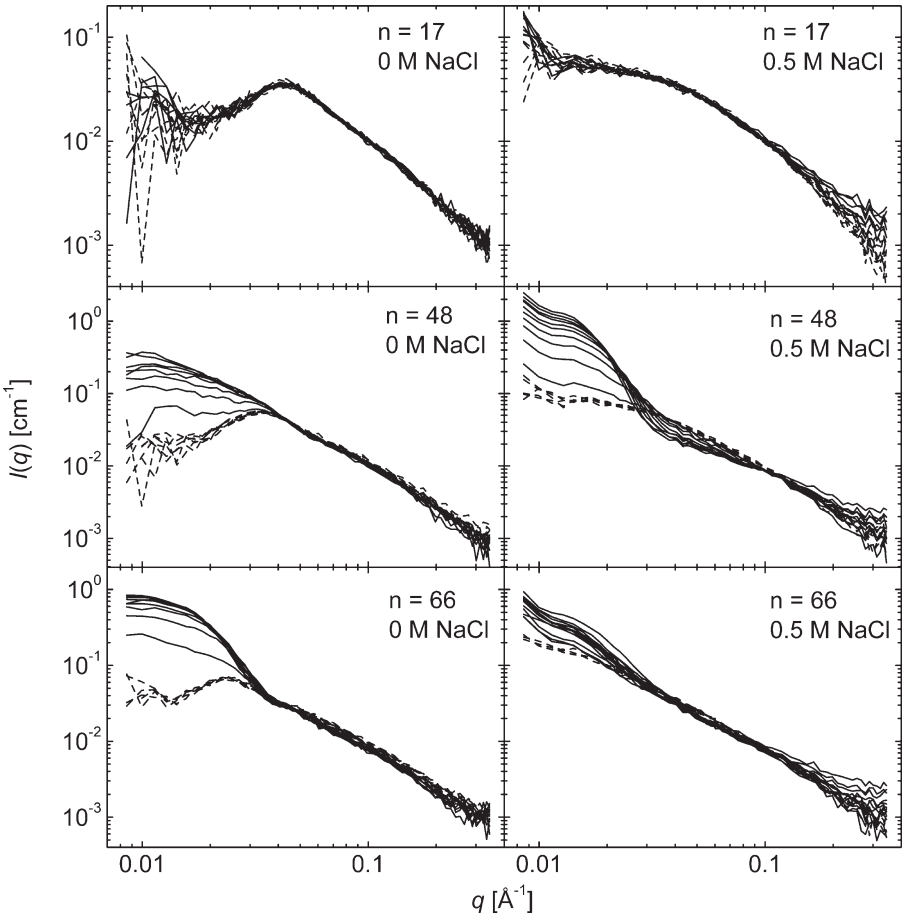

Figure 5. SAXS data from 1 wt % solutions of the $M(PEG)_{45}$-*b*-$P(NIPAAM)_n$-*b*-$P(SSS)_{22}$ samples at various temperatures in the interval 20−90 °C and at the salt levels indicated. The data in the range 20 to 60 °C are shown as broken curves and from 65 to 90 °C as full curves.

PNIPAAM block (n = 17) is not affected by temperature at any level of salt addition. This suggests that, if any large clusters are formed, they are swollen in water with a low value of n_p/n_0. In the absence of salt the turbidity is practically independent of temperature over the considered temperature interval for all copolymers, except the copolymer with the longest (n = 66) PNIPAAM block, where a close inspection of the data divulges a transition peak with a maximum located at 40 °C (see inset plot in Figure 4c). The latter behavior has been reported[8,16,22] for other amphiphilic copolymers and was attributed to the formation of association complexes and their contraction at elevated temperatures.

As the length of the PNIPAAM block increases, the effect of salt addition on the temperature dependence of τ is more pronounced, particularly for the copolymer with the longest (n = 66) PNIPAAM sequence (Figure 4c). In this case, the temperature-induced turbidity rises strongly with salt addition and at higher salinity the cloudiness of the solutions is easily registered by the naked eye. Actually, at the highest salt concentration (2 M) the polymer cannot be dissolved. The results indicate that screening of the electrostatic interactions in combination with the salting-out effect (see the discussion below) at high salinity of the copolymer with long PNIPAAM sequences lead to high stickiness and flocculation of the species. It has recently been observed[14] for homo-PNIPAAM that long chains favor the intensity of the temperature-induced aggregation of PNIPAAM chains.

At low salt concentration, the screening of the electrostatic interactions is the dominating factor but, as the level of NaCl addition is increased, the salt may increase the strength of the hydrophobic interactions.[44−46] In the so-called "Hofmeister series",[47,48] Cl^- ions are classified as kosmotropes (structure makers) and they can enhance the hydrophobicity of the solute[45] and this may lead to salting-out effect of the polymer and macroscopic phase separation. In a previous study,[44] the effect of a series of sodium salts on the lower critical solution temperature (LCST) of PNIPAAM was investigated and it was found that addition of NaCl lowers the LCST by destabilizing the hydrophobic hydration of the polymer. The results revealed that all the effects of Hofmeister anions on PNIPAAM solvation could be explained in terms of three types of interactions of the ions with the polymer and its hydration waters. First, the anions can induce polarization of water molecules that are involved in hydrogen bonding with the amide. Second, the anions can obstruct the hydrophobic hydration of the polymer by increasing the surface tension of the cavity surrounding the backbone and the isopropyl side chains. Third, the anions may bind directly to the polyamide. It was argued[44] that the two first types of interactions should lead to salting-out of the polymer and thereby lowering the LCST, whereas the third effect, which is not important for NaCl, generates salting-in of the polymer.

The inset plot in Figure 4b illustrates the effect of temperature on the turbidity for 1 wt % solution of the uncharged diblock copolymer $MPEG_{45}$-*b*-$PNIPAAM_{48}$ with the same lengths of the

dx.doi.org/10.1021/jp1075884 |*J. Phys. Chem. B* 2011, 115, 2125–2139

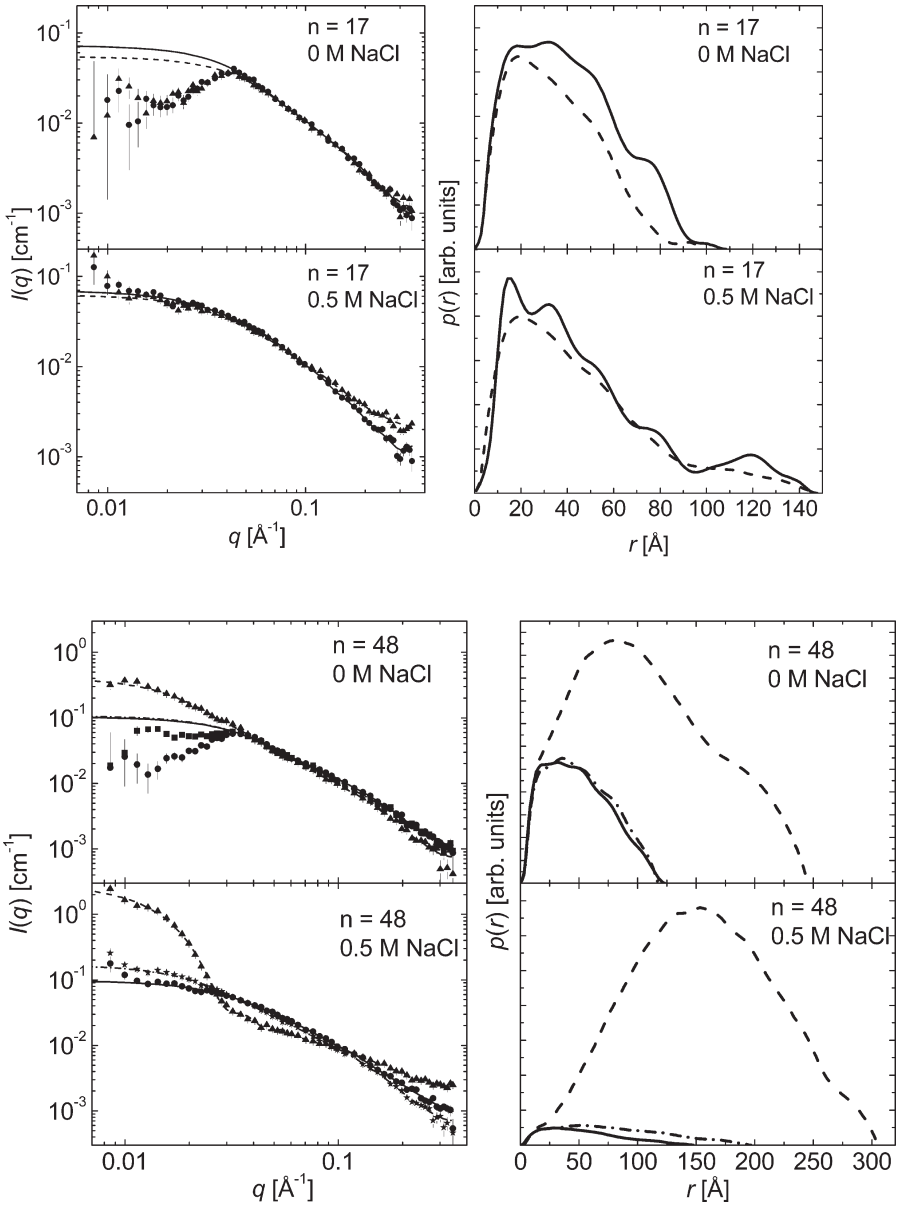

Figure 6. SAXS data and the pair distance distribution function $p(r)$ for 1 wt % solutions of $M(PEG)_{45}$-*b*-$P(NIPAAM)_n$-*b*-$P(SSS)_{22}$ with $n = 17$ (upper panel) and $n = 48$ (lower panel). The lines in the left-hand side represent fits from the indirect Fourier transformation and correspond to the $p(r)$ functions shown at the right-hand side. For $n = 17$, solid circles and full curves are at 20 °C and solid triangle and dashed curves are at 90 °C. The same notation is used for $n = 48$ for these temperatures, and for the intermediate temperatures, the SAXS data without salt at 55 °C are shown as solid squares, and the data at 0.5 M salt at 45 °C are shown as solid stars. The corresponding fits and $p(r)$ functions are shown as dashed-dotted curves.

MPEG and PNIPAAM blocks as the corresponding charged triblock copolymer ($M(PEG)_{45}$-*b*-$P(NIPAAM)_{48}$-*b*-$P(SSS)_{22}$). However, even in salt-free solutions this polymer yields high turbidity values at elevated temperatures and this trend indicates pronounced interchain associations. This suggests that as the hydrophobicity of the NIPAAM chains rises with increasing temperature the hydrophilic MPEG chains are not stabilizing the PNIPAAM core because they are not sufficiently long to cover the PNIPAAM core effectively. This situation is interesting to compare with that for the corresponding triblock copolymer (Figure 4b) at a high level of salt addition (2 M NaCl) where all the charges of the polymer can safely be assumed to be screened. At this stage, one expects that all the phenyl groups from the PSSS block should contribute to the hydrophobicity of the polymer species, and this should promote aggregation at higher temperatures. However, the very low turbidity values, even at high temperatures, tell us that if aggregates are present in this sample, they have a much more open structure than what is observed for the corresponding diblock copolymer. For the sample with the longest ($n = 66$) PNIPAAM chains, the cores formed in the presence of high levels of salt addition are too large to be covered by MPEG chains and this leads to interparticle aggregation at elevated temperatures (Figure 4c). In addition, it is known that high NaCl concentration promotes augmented turbidity at high temperatures due to salting-out effects or more intense hydrophobicity of the PNIPAAM entities[44] and thereby high sticking affinity of the particles. This leads to macroscopic phase separation at the highest salt concentration (2 M NaCl).

dx.doi.org/10.1021/jp1075884 |*J. Phys. Chem. B* 2011, 115, 2125–2139

The temperature at which the first deviation of the scattered intensity from the baseline occurred was taken as the cloud point, and it is evident from Figure 4d that the value of the cloud point drops with rising length of the PNIPAAM block and increasing salinity. This clearly illustrates that both block size and salinity promote macroscopic aggregation of the copolymer. It has been reported for aqueous solutions of the homopolymer PNIPAAM that both increasing length[14,34,49,50] of the PNIPAAM block and salinity[44,46] lead to depression of the cloud point.

SAXS Results. Figure 5 shows SAXS data at temperatures between 20 and 90 °C in steps of 5 °C for 1 wt % solutions of $M(PEG)_{45}$-*b*-$P(NIPAAM)_n$-*b*-$P(SSS)_{22}$ with and without added salt. For the copolymer with the shortest PNIPAAM block ($n = 17$), the scattering curves representing various temperatures collapse onto each other, both for the solution with and without added salt. The fact that no influence of temperature can be traced in the scattering curves at low q values suggests that interchain association can be neglected, even when salt is added. This behavior is consistent with the results from the turbidity measurements on this sample. Another conspicuous feature is the interaction peak observed at intermediate q values for the sample in the absence of salt. We notice that the interaction peak disappears in the presence of salt. SAXS is sensitive to structures with length scales of order $2\pi/q$ and the mean interaggregate or interchain distance d can be estimated from $d = 2\pi/q_{max}$, where q_{max} is the location of the maximum of the peak. The maximum is centered at $q_{max} = 0.045$ Å^{-1} and this corresponds to $d = 433$ Å. An interaction peak in the intermediate q domain has been reported for many other systems with polyelectrolyte character[51−55] and this behavior can be attributed to electrostatic interactions and the formation of more or less ordered arrangement of ionic structures. Previous scattering investigations[51−53,55] on polyelectrolyte systems have revealed that the height of the peak in the scattered intensity decreases gradually with increasing salt concentration, and at sufficient high level of salt addition, the peak disappears and the scattering profile resembles that of a neutral polymer.

The scattered intensity curves exhibit a different profile for the samples with $n = 48$ and $n = 66$ (Figure 5). In this case, a temperature-induced separation of the curves takes place at low q values and this effect is ascribed to chain aggregation. For the salt-free solutions, it is possible to discern an interaction peak at intermediate q values at low temperatures, but this peak disappears at higher temperatures. This behavior reflects the delicate competition between electrostatic interactions in terms of repulsion and enhanced hydrophobic associations at elevated temperatures. At low temperatures the scattered intensity curves condense onto each other over the full q range, but at a certain temperature an incipient separation of the curves occurs. This provides a rough estimate of the critical micelle temperature (cmt) and it decreases with increasing length of the PNIPAAM block and upon addition of salt. This finding is in agreement with the trend observed for the value of the cloud point under these conditions. The results suggest that the separation of the curves is interrelated to the macroscopic aggregation of the polymer species.

Figure 6 shows the scattered intensity curves for 1 wt % solutions of $M(PEG)_{45}$-*b*-$P(NIPAAM)_n$-*b*-$P(SSS)_{22}$ with $n = 17$ (upper panel) and $n = 48$ (lower panel), together with the corresponding pair distance distribution functions $p(r)$ obtained by IFT with and without added salt at the temperatures indicated. The forward scattering was calculated from $p(r)$ and for the lowest temperatures this gives the average values $I(0) = 0.058$, 0.090, and 0.105 cm^{-1} for the polymers with $n = 17$, 48 and 66, respectively. The relative values of these compared to that of the $n = 66$ polymer are 0.55, 0.86, 1.00, which are very close to the corresponding relative masses of polymers, which are 0.57, 0.86, and 1.00. Considering the relation for the forward scattering $I(0) = cM_w\Delta\rho^2$, where $\Delta\rho$ is the excess scattering length of the polymer per unit mass, this is, when there are small variations in $\Delta\rho$ between the polymers, in agreement with absence of association of the polymers at 20 °C.

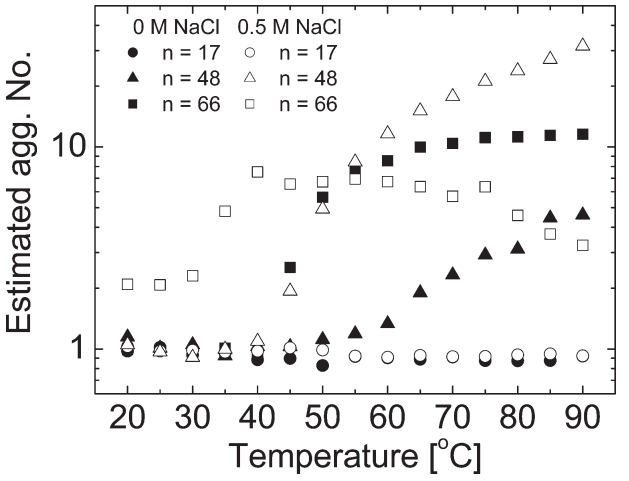

Figure 7. Aggregation numbers of the polymers estimated from the forward scattering derived from the SAXS data.

The forward scattering was used for calculating an estimate of the aggregation number N_{agg} of the solutions as described in Theory and Data Analysis and the values are displayed in Figure 7. For the copolymer with $n = 17$, the influence of temperature on the $p(r)$ function is modest, both for the solution with and without added salt. With our estimate that $\Delta\rho^2$ changes by at most a factor of 2 between the lowest and the highest temperature, this is consistent with a nearly constant value of the aggregation number with $N_{agg} \approx 1-2$. These results suggest that, when the PNIPAAM unit is small, both the temperature- and salt-induced aggregations are repressed. For the sample with $n = 48$, the $p(r)$ function becomes broader and the maximum is shifted to longer distances as the temperature is increased. Addition of salt to the sample strengthened these effects. These findings, together with the large values of N_{agg} at higher temperatures, demonstrate that augmented chain aggregation is promoted by raising the temperature and upon addition of salt. We note that, in the absence of salt, the effect of temperature on the $p(r)$ curve is small all the way up to 55 °C and $N_{agg} \approx 1$.

For the copolymer with the longest PNIPAAM block ($n = 66$), a more intricate picture emerges (Figure 8). In the copolymer solution without salt, a strong temperature effect of the $p(r)$ function is already observed at 35 °C, which parallels the turbidity changes for this sample. This supports the previous findings that the copolymer with a large PNIPAAM unit is more inclined to form aggregates at lower temperatures than the copolymers with small PNIPAAM units. In the presence of salt, a more complex behavior appears with low values of N_{agg}, in spite of the fact that the turbidity measurements show strong flocculation or aggregation effects. The IFT gives a maximum diameters of about 30 nm, however, as the DLS measurements (see below) give apparent hydrodynamic radii of about 100 nm above 35 °C

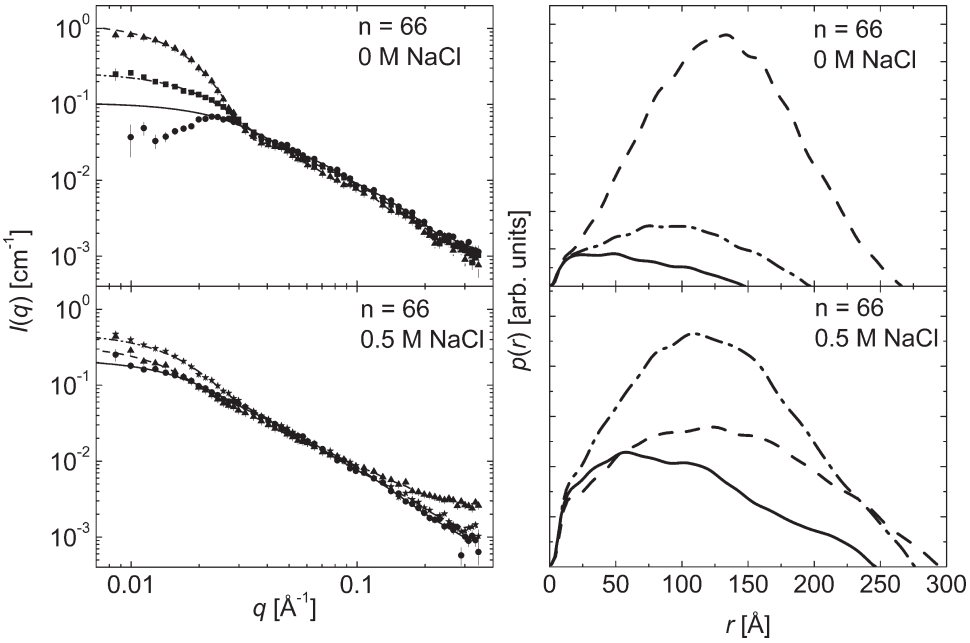

Figure 8. SAXS data, the pair distance distribution function $p(r)$ for 1 wt % solutions of $M(PEG)_{45}$-*b*-$P(NIPAAM)_n$-*b*-$P(SSS)_{22}$ with n = 66 at the temperatures and levels of salt addition indicated. The solid lines represent fits from the indirect Fourier transformation and correspond to the $p(r)$ functions shown on the right-hand side. The lines in the left-hand side represent fits from the indirect Fourier transformation and correspond to the $p(r)$ functions shown on the right-hand side. Solid circles and full curves are at 20 °C and solid triangles and dashed curves are at 90 °C. For the intermediate temperatures, the SAXS data without salt at 45 °C are shown as solid squares, and the data at 0.5 M salt at 35 °C are shown as solid stars. The corresponding fits and $p(r)$ functions are shown as dashed-dotted curves.

both with and without salt; this suggests that it is only a substructure that is observed by SAXS. It can be the cross-section structure of elongated micelles of subparticles of a larger cluster. The SAXS measurements do not go to small enough scattering vectors to give information of the larger structures.

Figure 9 shows plots of $I(q)$ versus q for 1 wt % solutions of $M(PEG)_{45}$-*b*-$P(NIPAAM)_n$-*b*-$P(SSS)_{22}$ in the presence of salt (0.5 M NaCl) at a temperature of 20 °C. These scattering data appear to be similar to those of noncharged, singly dissolved polymer chains. For the samples with n = 17 and n = 48, the scattered intensity data have been fitted with the aid of the Debye function (1) and values of R_g have been determined to, respectively, 33.2 ± 0.5 and 43.6 ± 0.6 Å. The data are well fitted by the Debye function and we note that the value of R_g is larger for the copolymer with a larger PNIPAAM block. For the copolymer with n = 66, we tried a similar approach, although the values determined for the aggregation numbers show that this polymer is slightly aggregated with $N_{agg} \approx 2$ already at low temperatures. The quality of the fit for the Gaussian chain model was poor. However, the expression given by Pedersen and Schurtenberger[29] for chains with excluded volume effects could be used. With this model, the scattered intensity data for the copolymer with n = 66 can be well fitted (see Figure 9c) and the fit yields a value of R_g = 79 ± 3 Å. It is well-known[56] that for longer chains the excluded volume effect is more developed. For Gaussian we have the simple relation (3) for the radius of gyration. With an estimate of the contour length L of the polymer, it can be used for determining the Kuhn length b. L can be estimated as (1.5 Å) × number of C−C and C−O bonds in the backbone of the polymer. For the n = 17, polymer $L \approx$ 324 Å and the R_g value gives b = 20 Å which is close to values for similar polymers.[57]

The Kuhn length of 27 Å for the n = 48 polymer is in reasonable agreement. For the n = 66 we observe excluded volume effects as well as aggregation with $N_{agg} \approx 2$ and both points have to be taken into account. We use[58] $\langle R_g^2 \rangle \approx (L/b)^{1.18} b^2/6$ and simply estimate the contour length to be twice that of a single chain and obtain a Kuhn length of 20 Å in very good agreement with the value for the n = 17 polymer.

Dynamic Light Scattering Results. Figure 10 shows some typical time correlation function data (at a scattering angle of 90°) for 1 wt % solutions of $M(PEG)_{45}$-*b*-$P(NIPAAM)_n$-*b*-$P(SSS)_{22}$ (n = 17) at different levels of salt addition and various temperatures, together with some curves fitted with the aid of (10). By plotting the correlation function data against the quantity tT/η, trivial changes of the solvent viscosity with temperature have been taken into account. The decay of the correlation function reveals effects of both temperature and salinity. As mentioned above, the fitting procedure yields at most of the conditions a fast and a slow relaxation mode. From the fast relaxation (always diffusive), the apparent hydrodynamic radius can be calculated for the small species, whereas from the non-diffusive slow relaxation mode the reduced relaxation time is determined for the larger species. Interestingly, even though no significant temperature effect is observed for the polymer with the shortest PNIPAAM block from either turbidity or the SAXS experiments, the correlation functions are clearly temperature dependent for this polymer both in the presence and absence of added salt.

Figure 11 shows the temperature dependences of the apparent hydrodynamic radius, calculated from the fast relaxation mode, for 1 wt % solutions of $M(PEG)_{45}$-*b*-$P(NIPAAM)_n$-*b*-$P(SSS)_{22}$ with different levels of salt addition. Let us first discuss the results for the copolymer with the shortest PNIPAAM block. In the absence of added salt, the apparent R_h is virtually independent of temperature and the size of the species is small (R_h < 1 nm). There is strong influence from electrostatic repulsion in this

dx.doi.org/10.1021/jp1075884 |*J. Phys. Chem. B* 2011, 115, 2125–2139

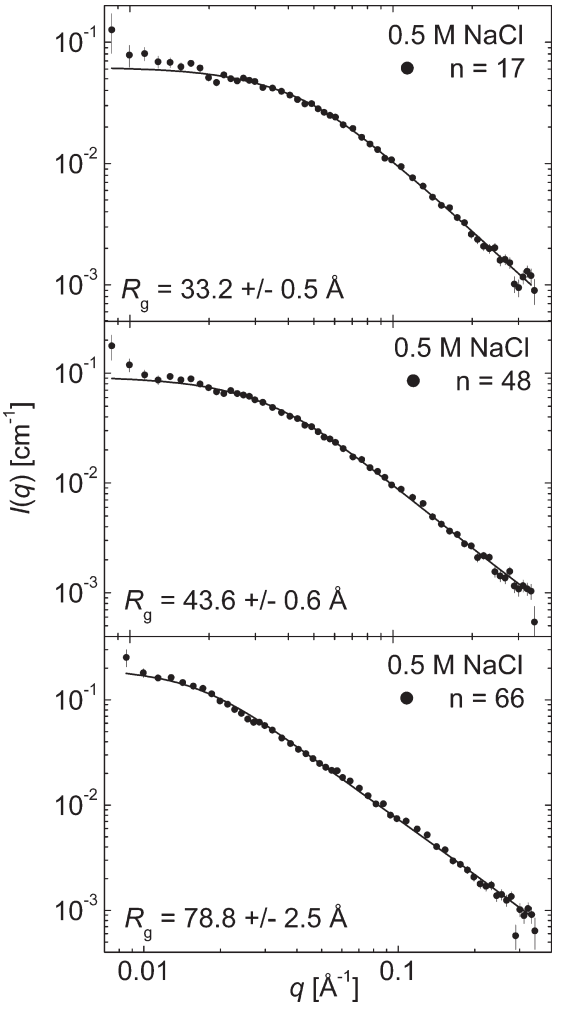

Figure 9. Scattering functions for 1 wt % solutions of $M(PEG)_{45}$-*b*-$P(NIPAAM)_n$-*b*-$P(SSS)_{22}$ in the presence of 0.5 M NaCl at 20 °C. The fitted curves have been constructed with the aid of (1) and a numerical expression given in ref 29 for flexible chains with excluded volume effects.

region. Upon addition of salt, a larger value of R_h is observed and this is probably due to the screening of electrostatic repulsion. Similar effects are observed[59] for homopolymer polyelectrolytes. At 25 °C in 0.5 M salt, the value is 3.9 nm, which is comparable to the radius of gyration determined by SAXS. At the highest salinity, the value of R_h increases at high temperatures because of the enhanced hydrophobicity of the solute in the presence of salt and the associated aggregation of the polymer.

For the samples with $n = 48$, a sharp transition to higher values of R_h is found at about 50 °C for the sample without added salt. This feature indicates that micelles are formed at elevated temperatures. In the presence of 0.5 M NaCl, the transition is smoother and it starts at a much lower temperature than for the sample without salt. This is ascribed to screening of electrostatic interactions and salting-out effects. At a salt concentration of 1.0 M, the fast relaxation mode disappears at ca. 35 °C, and in the presence of 2.0 M NaCl the fast mode cannot be observed in the considered temperature region. This is due to the strong dominance of the large species that are probed by the slow relaxation mode. For the sample with $n = 66$ without added salt, a similar sharp transition of R_h as for $n = 48$ is also detected, but in this case the transition is shifted to a much lower temperature (ca. 38 °C) because of the higher hydrophobicity of this polymer. When 0.5 M NaCl is added to the solution, the progressive transition starts at a lower temperature, which again shows that salt addition promotes augmented hydrophobicity of the polymer. For the sample with $n = 66$, the slow relaxation mode dominates the correlation function at 1.0 M NaCl, and no fast mode can be observed. This sample does not dissolve in 2.0 M NaCl even at low temperatures.

Figure 12 illustrates the effects of temperature and salt addition on the reduced slow relaxation time for 1 wt % solutions of $M(PEG)_{45}$-*b*-$P(NIPAAM)_n$-*b*-$P(SSS)_{22}$ for the polymers with different values of *n*. Since this mode is not always diffusive as the fast mode but exhibits stronger *q* dependence at some conditions, the results are presented in terms of a reduced relaxation time, where trivial changes of the solvent viscosity with temperature have been taken into account. In the solutions of these copolymers, the dynamics of large interchain complexes or intermicellar structures coexist with diffusion of unimers and micelles. Since the slow mode relaxes at much longer times than the fast mode, this suggests that the slow mode essentially probes the dynamics of large species. In 0.5 M NaCl, the slow mode of the sample with $n = 17$ is diffusive at 60 °C (see Figure 13b). At these conditions, the radius calculated from the fast mode is about 4 nm while the radius calculated from the slow mode is about 220 nm, confirming that the appearance of the slow mode is due to the presence of large aggregates in the solution.

In the solution of the polymer with the shortest PNIPAAM block (Figure 12a) without salt addition, swelling of the polymer aggregates caused by electrostatic repulsions causes the value of the reduced slow relaxation time at low temperatures to be significantly higher than for the corresponding ones in the presence of salt. At elevated temperatures, the sample without salt contracts due to the enhanced hydrophobicity of the PNIPAAM blocks. For the samples containing salt, one would also expect this contraction to occur. However, since most of the electrostatic repulsive forces are screened, there is also an aggregation of the polymer clusters, causing an overall increase of the reduced slow relaxation time. Interestingly, these samples exhibit a very low and constant turbidity (see Figure 4a). This indicates that even though large aggregates are present in these samples, they have a relatively open structure. This is probably caused by the very short PNIPAAM group which is located in the middle of the triblock copolymer. The core of the aggregates cannot contain only PNIPAAM groups, since steric hindrance prevent the copolymer from bending enough for such a conformation. Having a core consisting of not only PNIPAAM but also a significant amount of hydrophilic groups prevent the microphase separation that usually induce the enhanced turbidity values observed for PNIPAAM containing polymers at elevated temperatures.

For the sample with $n = 48$, a similar behavior as for $n = 17$ is observed in the absence of salt, but in this case the transition is shifted to a lower temperature. For this sample, a reduction of the reduced slow relaxation time at elevated temperatures is also observed for the lower two salt concentrations. The flexibility of the PNIPAAM chain increases as it becomes longer, and the core of the aggregates contains more PNIPAAM and less of the hydrophilic blocks than that of the $n = 17$ copolymer. It is therefore easier for the aggregates to contract, and in the competition between contraction and aggregation, the contraction dominates at intermediate temperatures. At the highest salt concentration (2 M NaCl), only a modest increase of the reduced

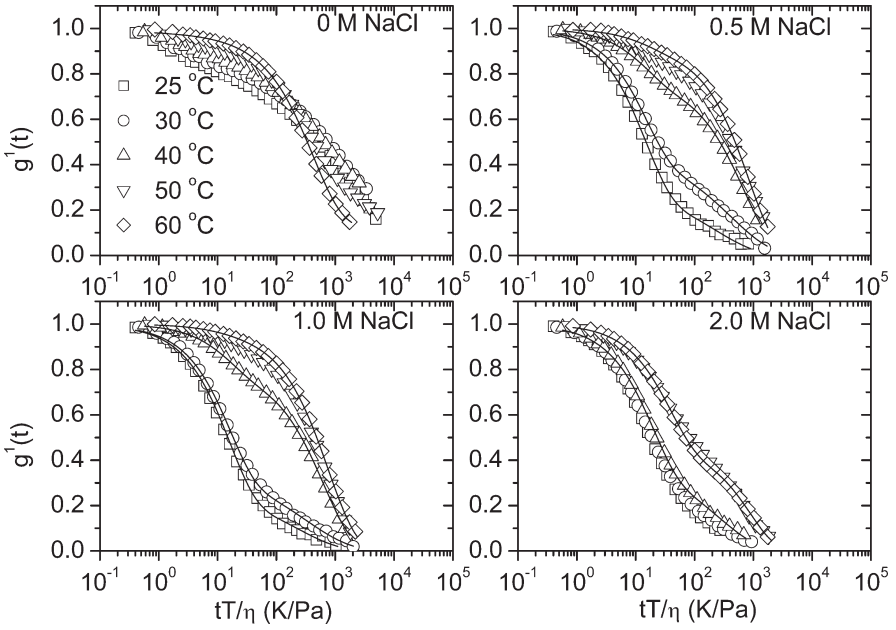

Figure 10. First-order correlation functions (at a scattering angle of 90°; every third point is shown) versus the quantity tT/η (trivial changes of the solvent viscosity with temperature are thereby accounted for) for 1 wt % solutions of $M(PEG)_{45}$-*b*-$P(NIPAAM)_{17}$-*b*-$P(SSS)_{22}$ at the temperatures and salinities indicated. The lines are fitted with the aid of eq 10.

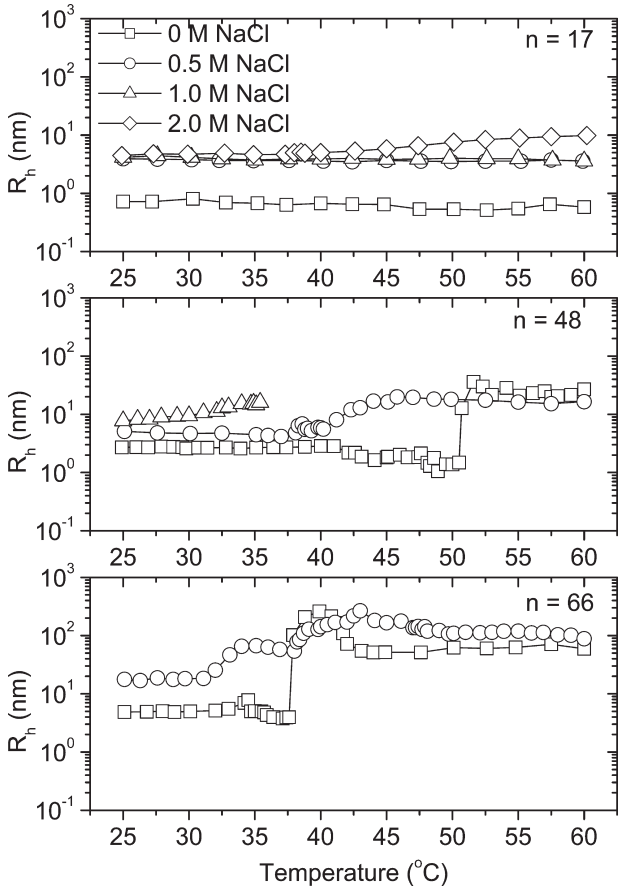

Figure 11. Temperature dependences of the apparent hydrodynamic radius, calculated from the fast relaxation mode, for 1 wt % solutions of $M(PEG)_{45}$-*b*-$P(NIPAAM)_n$-*b*-$P(SSS)_{22}$ in the presence of various levels of salt addition. See text for details.

slow relaxation time with temperature is observed, because at this stage of high level of salt addition the intermicellar structures are strongly compressed even at low temperatures by the salt-induced amplified hydrophobicity of the species.

For the sample with the longest PNIPAAM block, a more intricate feature is observed (Figure 12c) both with and without salt. In the absence of salt, the contraction that is observed for the n = 17 and the n = 48 samples is shifted toward even lower temperatures, but in this case it is followed by a peak at intermediate temperatures. This behavior reflects the competition between the temperature-induced contraction of large interchain complexes with many PNIPAAM segments and interchain aggregation as the temperature rises. This type of behavior has been reported[16,22] previously for aqueous solutions of charged block copolymers containing PNIPAAM. The peak at about 40 °C is also reflected in the turbidity data (inset in Figure 4c). For the sample with 0.5 M NaCl, we note again that at low temperatures the intermicellar structures are strongly condensed because of the enhanced hydrophobicity of the species in the presence of salt. At intermediate temperatures, large aggregation complexes are formed and these aggregates are compacted at higher temperatures. As observed for the sample without salt, these changes are reflected in the turbidity values (Figure 4c). This indicates that, when the PNIPAAM block is long enough to become more flexible, the polymers in the clusters can be arranged so that the core mostly consists of the PNIPAAM block. At elevated temperatures, this core contracts enough to induce enhanced turbidity values. At high salinity (1 M NaCl), there is an initial increase in the reduced slow relaxation time at low temperatures followed by a slight decrease before it flattens out at high temperatures. At high temperatures, the reduced slow relaxation time for the sample with 1.0 M NaCl is lower than that observed for the sample with 0.5 M NaCl, even though the turbidity values are much higher for the sample that contains

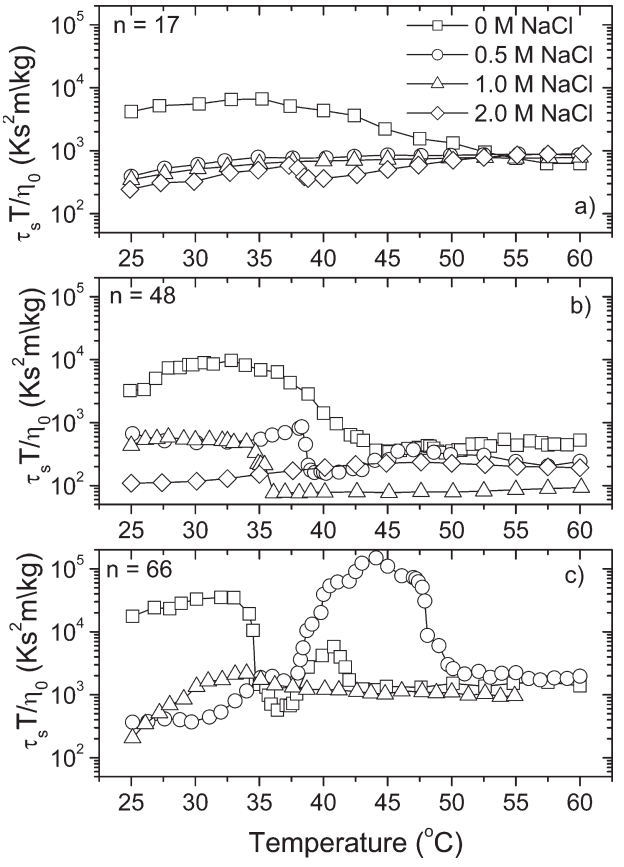

Figure 12. Effects of temperature and salt addition on the reduced slow relaxation time for 1 wt % solutions of $M(PEG)_{45}$-*b*-$P(NIPAAM)_n$-*b*-$P(SSS)_{22}$. See text for details.

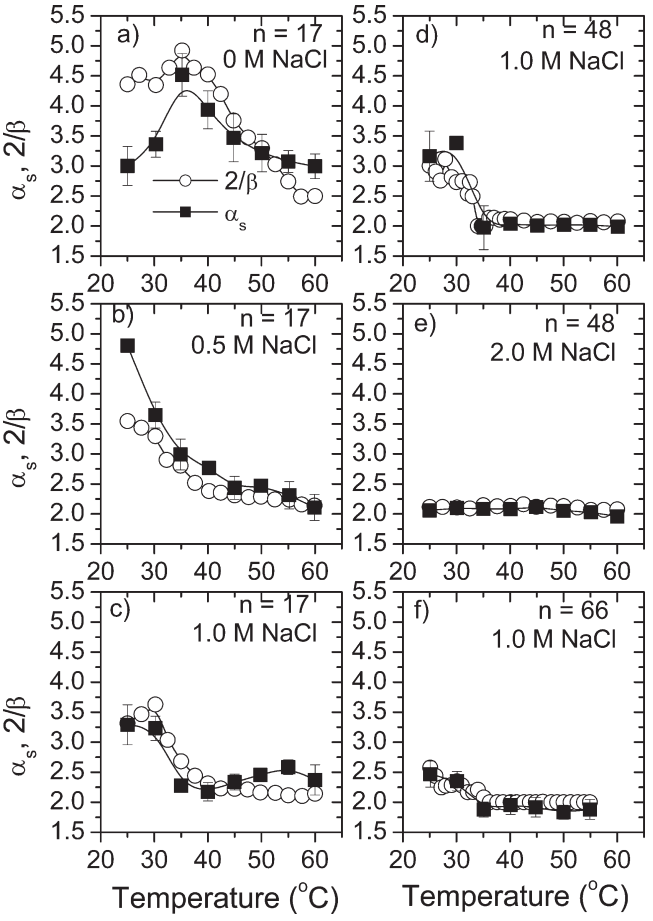

Figure 13. Effects of temperature and salt addition on the quantities 2/β (see text for explanation) and α_s, expressing the q dependence of the slow relaxation time, for 1 wt % solutions of $M(PEG)_{45}$-*b*-$P(NIPAAM)_n$-*b*-$P(SSS)_{22}$.

most salt. This suggests that very compact clusters are formed for this polymer at high salt concentrations.

The q dependences of the inverse fast and slow relaxation times can be expressed as $\tau_f^{-1} \propto q^{\alpha_f}$ and $\tau_s^{-1} \propto q^{\alpha_s}$, respectively. The fast mode is always diffusive ($\alpha_f = 2$), while the slow relaxation mode exhibits an anomalous q dependence. The q dependence of the slow mode can be interpreted in the framework of the coupling approach elaborated by Ngai and coworkers.[60−62] This model deals with the problem of how the relaxation of a specific chain or cluster is slowed due to the coupling to complex surroundings, and this approach has been employed in the analysis of dynamical features in associating and gelling polymer systems of various natures.[63−68] The results of the slow relaxation time and the stretched exponential β can be interrelated and rationalized by the coupling model, which is semiempirical in the sense that it does not identify the particular mechanism or the exact nature of the interaction responsible for the coupling. The basic prediction of this model is that the coupling parameter m ($0 \leq m < 1$) rises (or the stretched exponent β decreases) as the coupling strength between the species is increased. In this framework, the parameter m ($\beta = 1 - m$), the effective slow relaxation time τ_s^*, the characteristic time for unconstrained relaxation τ_0, and the crossover time t_c are linked to each other through the expression

$$\tau_s^* = [t_c^{\beta - 1}\tau_0]^{1/\beta} \qquad (15)$$

The value of β is a direct measure of the coupling strength of the slow relaxation mode to its complex surroundings. A decreasing value of β indicates enhanced coupling effects and (15) predicts longer relaxation times. The general behavior of the reduced slow relaxation time at various conditions is consistent with the trend of β.

Another intrinsic property of the coupling model is the prediction[60] of the anomalous q dependence of the slow relaxation time through the relationship

$$\tau_s^* = [t_c^{-m}\tau_0(q)]^{1/(1-m)} \propto q^{-2/(1-m)} \propto q^{-2/\beta} \qquad (16)$$

It is obvious from the above equation that, as the coupling or interaction in the solution is enhanced, there is a concomitant increase in the value of m, or a decrease of β, and the q dependence of τ_s becomes stronger than that of a diffusive process. A comparison between the experimental results and the values determined with the aid of (16) is depicted in Figure 13. The overall picture that emerges is that the agreement between the experimentally determined values and the calculated ones is good. For the block copolymer with the shortest PNIPAAM sequence ($n = 17$) (Figure 13a−c), the value of α_s drops as the temperature increases, both with and without added salt, and this may indicate that loose interconnected structures are formed at low temperatures, whereas compressed nonconnected species are developed at high temperatures. An inspection of the results reveals that elevated temperatures and salt addition favor diffusion behavior ($\alpha_s = 2$) of the slow relaxation process.

dx.doi.org/10.1021/jp1075884 |*J. Phys. Chem. B* 2011, 115, 2125–2139

Our conjecture is that the interchain structures are compressed and stabilized by MPEG chains so there are no strong intermolecular interactions between the species.

CONCLUSIONS

In this work, effects of temperature and salt addition on the association behavior of aqueous solutions of charged triblock copolymers $MPEG_{45}$-*b*-$P(NIPAAM)_n$-*b*-$P(SSS)_{22}$ containing different lengths of the PNIPAAM block (n = 17, 48, and 66) have been examined. The results from turbidimetry, SAXS, and DLS on solutions of the triblock copolymer show that increasing the length of the PNIPAAM block, as well as increasing temperature and/or salinity, results in the formation of interchain complexes.

The cloud point decreases with increasing value of n and rising level of salt addition, and this is compatible with the significantly higher values of the aggregation number observed from SAXS under these conditions. In salt-free solutions, the SAXS results reveal an interaction peak in the scattered intensity profile at intermediate q values, which is typical for electrostatic repulsion in polyelectrolyte solutions. This peak disappears at elevated temperatures and/or upon salt addition. The SAXS data from solutions of the copolymer with n = 66 indicate that in the presence of salt a substructure is probed, and not the global aggregated structures observed by turbidity and DLS. For solutions of the copolymers in the presence of 0.5 M NaCl, the q dependence of the SAXS intensity can be described by the Gaussian chain model for n = 17 and n = 48, whereas for n = 66, a model taking into account excluded volume effects provided the best fit of the data.

The fast mode from DLS clearly shows the formation of association complexes at elevated temperatures for solutions of the copolymers with n = 48 and n = 66. This effect is strengthened as the level of salt addition is increased. Analysis of the correlation functions disclosed a fast relaxation mode that always is diffusive and a slow relaxation mode that exhibits stronger anomalous q dependence. The latter behavior can be rationalized in terms of the coupling model of Ngai.

The findings from this study have demonstrated the delicate interplay between electrostatic repulsive forces and hydrophobic interactions. By changing the temperature, salinity, and the length of the PNIPAAM block, the strength of the associations can be tuned.

ACKNOWLEDGMENT

B.N. and K.Z. gratefully acknowledge support from the Norwegian Research Council for the project (177665/V30). M.A.B. and J.S.P. gratefully acknowledge the support from The Danish Council for Independent Research in Natural Sciences.

REFERENCES

(1) Muthukumar, M.; Ober, C. K.; Thomas, E. L. *Science* **1997**, *277*, 1225.
(2) Qiu, X.; Wu, C. *Macromolecules* **1997**, *30*, 7921.
(3) Förster, S.; Antonietti, M. *Adv. Mater.* **1998**, *10*, 195.
(4) Sommer, C.; Pedersen, J. S. *Langmuir* **2005**, *21*, 2137.
(5) Kjøniksen, A.-L; Laukkanen, A.; Galant, C.; Knudsen, K. D.; Tenhu, H.; Nyström, B. *Macromolecules* **2005**, *38*, 948.
(6) *Responsive Polymer Materials: Design and Applications*; Minko, S., Ed.; Blackwell Publishing: Ames, IA, 2006.
(7) *Block Copolymers in Nanoscience*; Lazzari, M., Liu, G., Lecommandoux, S., Eds.; Wiley-VCH: Weinheim, Germany, 2006.
(8) Zhu, K.; Jin, H.; Kjøniksen, A.-L.; Nyström, B. *J. Phys. Chem. B* **2007**, *111*, 10862.
(9) Zhu, K.; Pamies, R.; Kjøniksen, A.-L.; Nyström, B. *Langmuir* **2008**, *24*, 14227.
(10) Bertrand, N.; Fleischer, J. G.; Wasan, K. M.; Leroux, J.-C. *Biomaterials* **2009**, *30*, 2598.
(11) Wei, H.; Cheng, S.-X.; Zhang, X.-Z.; Zhuo, R.-X. *Prog. Polym. Sci.* **2009**, *34*, 893.
(12) Chuang, C.-Y.; Don, T.-M.; Chiu, W.-Y. *J. Polym. Sci. (Part A)* **2009**, *47*, 5126.
(13) Schild, H. K. *Prog. Polym. Sci.* **1992**, *17*, 163.
(14) Pamies, R.; Zhu, K.; Kjøniksen, A.-L.; Nyström, B. *Polym. Bull.* **2009**, *62*, 487.
(15) Halperin, A. *Macromolecules* **1990**, *23*, 2724.
(16) Kjøniksen, A.-L.; Zhu, K.; Pamies, R.; Nyström, B. *J. Phys. Chem. B* **2008**, *112*, 3294.
(17) Wang, J. S.; Matyjaszewski, K. *J. Am. Chem. Soc.* **1995**, *117*, 5614.
(18) Matyjaszewski, K.; Xia, J. *Chem. Rev.* **2001**, *101*, 2921.
(19) Ciampolini, M.; Nardi, N. *Inorg. Chem.* **1966**, *5*, 41.
(20) Liu, S.; Weaver, J. V. M.; Tang, Y.; Billingham, N. C.; Armes, S. P. *Macromolecules* **2002**, *35*, 6121.
(21) Matyjaszewski, K.; Tsarevsky, N. V. *Nat. Chem.* **2009**, *1*, 276.
(22) Kjøniksen, A.-L.; Zhu, K.; Karlsson, G.; Nyström, B. *Colloids Surf., A* **2009**, *333*, 32.
(23) Messaud, F. A.; Sanderson, R. D.; Runyon, J. R.; Otte, T.; Pasch, H.; Kim, S.; Williams, R. *Prog. Polym. Sci.* **2009**, *34*, 351.
(24) Pedersen, J. S. *J. Appl. Crystallogr.* **2004**, *37*, 369.
(25) Orthaber, D.; Bergmann, A.; Glatter, O. *J. Appl. Crystallogr.* **2000**, *33*, 218.
(26) Debye, P. *J. Phys. Colloid Chem.* **1947**, *51*, 18.
(27) Pedersen, J. S. *Adv. Colloid Interface Sci.* **1997**, *70*, 171.
(28) Pedersen, J. S. Modelling of Small-Angle Scattering Data from Colloids and Polymer Systems. In *Neutrons, X-Rays and Light*; Lindner, P., Zemb, T., Eds.; Elsevier: New York, 2002; pp 391−420.
(29) Pedersen, J. S.; Schurtenberger, P. *Macromolecules* **1996**, *29*, 7602.
(30) Glatter, O. *J. Appl. Crystallogr.* **1977**, *10*, 415.
(31) Pedersen, J. S.; Svaneborg, C.; Almdal, K.; Hamley, I. W.; Young, R. N. *Macromolecules* **2003**, *36*, 416.
(32) Sommer, C.; Pedersen, J. S.; Stein, P. C. *J. Phys. Chem. B* **2004**, *108*, 6242.
(33) Chiang, W.-H.; Hsu, Y.-H.; Chern, C.-S.; Chiu, H.-C. *J. Phys. Chem. B* **2009**, *113*, 4187.
(34) Siegert, A. J. F. Massachusetts Institute of Technology, Rad. Lab. Rep. No. 465, 1943.
(35) Kjøniksen, A.-L.; Nyström, B.; Tenhu, H. *Colloids Surf. A: Physicochem. Eng. Aspects* **2003**, *228*, 75.
(36) Chen, H.; Ye, X.; Zhang, G.; Zhang, Q. *Polymer* **2006**, *47*, 8367.
(37) Fleischer, G.; Puhlmann, A.; Rittig, F.; Konák, C. *Colloid Polym. Sci.* **1999**, *277*, 986.
(38) Vink, H. *J. Chem. Soc., Faraday Trans.I* **1985**, *81*, 1725.
(39) Selser, J. In *Light Scattering: Development and Principles*; Brown, W., Ed.; Clarendon Press: Oxford, UK, 1996; pp 232−254.
(40) *Block Copolymers in Nanoscience*; Lazzari, M., Liu, G., Lecommandoux, S., Eds.; Wiley-VCH: Weinheim, Germany, 2006.
(41) Rodriguez-Hernández, J.; Chécot, F.; Gnanou, Y.; Lecommandoux, S. *Prog. Polym. Sci.* **2005**, *30*, 691.
(42) Lechner, M. D. *J. Serb. Chem. Soc.* **2005**, *70*, 361.
(43) Al-Manasir, N.; Zhu, K.; Kjøniksen, A.-L.; Knudsen, K.; Karlsson, G.; Nyström, B. *J. Phys. Chem B* **2009**, *113*, 11115.
(44) Zhang, Y.; Furyk, S.; Bergbreiter, D. E.; Cremer, P. S. *J. Am. Chem. Soc.* **2005**, *127*, 14505.
(45) Zhang, Y.; Cremer, P. S. *Curr. Opin. Chem. Biol.* **2006**, *10*, 658.
(46) Zhang, Y.; Furyk, S.; Sagle, L. B.; Cho, Y.; Bergbreiter, D. E.; Cremer, P. S. *J. Phys. Chem. C* **2007**, *111*, 8916.

(47) Hofmeister, F. *Arch. Exp. Pathol. Pharmakol.* **1888**, *24*, 247.
(48) Kunz, W.; Henle, J.; Ninham, B. W. *Curr. Opin. Colloid Interface Sci.* **2004**, *9*, 19.
(49) Xia, Y.; Yin, X.; Burke, N. A. D.; Stöver, H. D. H. *Macromolecules* **2005**, *38*, 5937.
(50) Furyk, S.; Zhang, Y.; Ortiz-Acosta, D.; Cremer, P. S.; Bergbreiter, D. E. *J. Polym. Sci., Part A: Polym. Chem.* **2006**, *44*, 1492.
(51) Ermi, B. D.; Amis, E. J. *Macromolecules* **1997**, *30*, 6937.
(52) Borsali, R.; Nguyen, H.; Pecora, R. *Macromolecules* **1998**, *31*, 1548.
(53) Essafi, W.; Lafuma, F.; Williams, C. E. *Eur. Phys. J. B* **1999**, *9*, 261.
(54) Waigh, T. A.; Ober, R.; Williams, C. E.; Galin, J.-C. *Macromolecules* **2001**, *34*, 1973.
(55) Nishida, K.; Kaji, K.; Kanaya, T.; Shibano, T. *Macromolecules* **2002**, *35*, 4084.
(56) Weill, G.; Des Cloizeaux, J. *J. Phys. (Paris)* **1979**, *40*, 99.
(57) Fetters, L. J.; Lohsey, D. J.; Colby, R. H. In *Physical Properties of Polymers, Handbook*, 2nd ed.; Mark, J. E., Ed.; Springer Verlag: New York, 2007; pp 445−452.
(58) This equation agrees well with the simulation results in: Pedersen, J. S.; Laso, M.; Schurtenberger, P. *Phys. Rev. E* **1996**, *54*, R5817.
(59) Förster, S.; Schmidt, M; Antonietti, M. *Polymer* **1990**, *31*, 781.
(60) Ngai, K. L. *Adv. Colloid Interface Sci.* **1996**, *64*, 1.
(61) Rendell, R. W.; Ngai, K. L.; McKenna, G. B. *Macromolecules* **1987**, *20*, 2250.
(62) Ngai, K. L.; Rendell, R. W. *Philos. Mag. B* **1998**, *77*, 621.
(63) Nyström, B.; Walderhaug, H.; Hansen, F. K. *J. Phys. Chem.* **1993**, *97*, 7743.
(64) Nyström, B.; Lindman, B. *Macromolecules* **1995**, *28*, 967.
(65) Tsianou, M.; Kjøniksen, A.-L.; Thuresson, K.; Nyström, B. *Macromolecules* **1999**, *32*, 2974.
(66) Kjøniksen, A.-L.; Nilsson, S.; Thuresson, K.; Lindman, B.; Nyström, B. *Macromolecules* **2000**, *33*, 877.
(67) Tho, I.; Kjøniksen, A.-L.; Knudsen, K. D.; Nyström, B. *Eur. Polym. J.* **2006**, *42*, 1164.
(68) Beheshti, N.; Bu, H.; Zhu, K.; Kjøniksen, A.-L.; Knudsen, K. D.; Pamies, R.; Cifre, J. G. H.; de la Torre, J. G.; Nyström, B. *J. Phys. Chem. B* **2006**, *110*, 6601.